JOURNAL OF VIROLOGY, Mar. 2005, p. 3097–3106 Vol. 79, No. 5
0022-538X/05/$08.00+0 doi:10.1128/JVI.79.5.3097–3106.2005


# Recombinant Mouse Hepatitis Virus Strain A59 from Cloned, Full-Length cDNA Replicates to High Titers In Vitro and Is Fully Pathogenic In Vivo

Scott E. Coley,[1]†‡ Ehud Lavi,[2]†§ Stanley G. Sawicki,[3] Li Fu,[2] Barbara Schelle,[4] Nadja Karl,[4]¶ Stuart G. Siddell,[1]* and Volker Thiel[5]*

*Department of Pathology and Microbiology, School of Medical Sciences, University of Bristol, Bristol, United Kingdom[1]; Division of Neuropathology, Department of Pathology and Laboratory Medicine, School of Medicine, University of Pennsylvania, Philadelphia, Pennsylvania[2]; Department of Medical Microbiology and Immunology, Medical College of Ohio, Toledo, Ohio[3]; Institute of Virology and Immunology, University of Würzburg, Würzburg, Germany[4]; and Research Department, Cantonal Hospital St. Gallen, St. Gallen, Switzerland[5]*

Received 3 August 2004/Accepted 13 October 2004

**Mouse hepatitis virus (MHV) is the prototype of group II coronaviruses and one of the most extensively studied coronaviruses. Here, we describe a reverse genetic system for MHV (strain A59) based upon the cloning of a full-length genomic cDNA in vaccinia virus. We show that the recombinant virus generated from cloned cDNA replicates to the same titers as the parental virus in cell culture (~$10^9$ PFU/ml), has the same plaque morphology, and produces the same amounts and proportions of genomic and subgenomic mRNAs in virus-infected cells. In a mouse model of neurological infection, the recombinant and parental viruses are equally virulent, they replicate to the same titers in brain and liver, and they induce similar patterns of acute hepatitis, acute meningoencephalitis, and chronic demyelination. We also describe improvements in the use of the coronavirus reverse genetic system based on vaccinia virus cloning vectors. These modifications facilitate (i) the mutagenesis of cloned cDNA by using vaccinia virus-mediated homologous recombination and (ii) the rescue of recombinant coronaviruses by using a stable nucleocapsid protein-expressing cell line for the electroporation of infectious full-length genomes. Thus, our system represents a versatile and universal tool to study all aspects of MHV molecular biology and pathogenesis. We expect this system to provide valuable insights into the replication of group II coronaviruses that may lead to the development of novel strategies against coronavirus infections, including the related severe acute respiratory syndrome coronavirus.**

Coronaviruses (CoVs) are positive-strand enveloped RNA viruses that are associated mainly with respiratory and enteric infections (19). They have long been recognized as important pathogens of livestock and companion animals, and more recently, a coronavirus has been identified as the causative agent of severe acute respiratory syndrome (SARS), a form of atypical pneumonia in humans with a case/fatality ratio of ~10% (7, 8, 16, 27). Clearly, there is an urgent need to learn more about the natural history and pathogenesis of coronaviruses, as well as the molecular and cellular biology of coronavirus infections. In this respect, the prototype of the group II coronaviruses, murine hepatitis virus (MHV), seems to offer a number of advantages. It is commonly found in laboratory mice throughout the world and causes a wide spectrum of disease manifestations ranging from subclinical infections to high mortality, depending on the age, genotype, or immune status of the mice and the virus strain (1). The A59 strain of MHV (MHV-A59) was isolated in 1961 from a colony of BALB/c mice that was being used to serially propagate leukemia (22). There are a number of different animal disease models based upon MHV infection, including models of virus-associated demyelination and viral hepatitis (12, 18). These models provide important insights into the pathogenesis of virus infections. In addition, there is a wealth of genetic and immunological information relating to inbred mouse strains and there are an increasing number of transgenic mouse strains in which the expression of functional host cell genes is abolished or defective, particularly those encoding proteins related to the immunological response to virus infection. Therefore, MHV is an ideal tool to study both the innate and adaptive immune responses to viruses. In cell culture, MHV-A59 replicates to high titers, and there is a large collection of temperature-sensitive mutants that are defective in the synthesis of viral RNA (30). These features should facilitate the analysis of coronavirus RNA synthesis and the elucidation of functions associated with coronavirus replicase proteins. Finally, as the phylogenetic analysis of the SARS CoV genome has revealed a relationship to group II coronaviruses (32), the analysis of MHV infection may also help to elucidate some of the features of SARS coronavirus biology.

* Corresponding author. Mailing address for V. Thiel: Research Department, Cantonal Hospital St. Gallen, 9007 St. Gallen, Switzerland. Phone: 41-71-4941074. Fax: 41-71-4946321. E-mail: volker.thiel@kssg.ch. Mailing address for S. G. Siddell: Department of Pathology and Microbiology, School of Medical Sciences, University of Bristol, Bristol BS8 1TD, United Kingdom. Phone: 44-117-9287889. Fax: 44-117-9287896. E-mail: Stuart.Siddell@bristol.ac.uk.

† S.E.C. and E.L. contributed equally to this work.

‡ Present address: Department of Medicine, University of Massachusetts, Worcester, MA 01605.

§ Department of Pathology, Weill Medical College of Cornell University, New York, NY 10021.

¶ Present address: Rudolf-Virchow Center for Experimental Biomedicine, 97078 Würzburg, Germany.

The MHV genome is a large (31.4-kb) positive-strand RNA with a 5′ cap structure and a poly(A) tail. In the virion, the genome is associated with the nucleocapsid protein in a structure that lies within an envelope containing the membrane (M), envelope (E), and spike (S) proteins. Depending on the MHV strain, there may be an additional hemagglutinin esterase (HE) protein in the virion envelope (19). The packaging of MHV genomic RNA has been analyzed in detail and seems to be dependent on the interaction of the M protein and a packaging signal on the viral RNA (25). The cell tropism of MHV is determined mainly by the spike protein, which binds to the cellular receptor, CEACAM1 (37). After entry to the cell, the genomic RNA is used as mRNA for the translation of the replicase gene, which is located at the 5′ end of the viral RNA and encompasses about two-thirds of the genome. The resulting translation products, polyproteins 1a and 1ab, are proteolytically processed by virus-encoded proteases (two papain-like proteinases and the 3C-like proteinase) to generate products that form the viral replication and transcription complex (40). Viral RNA synthesis includes the replication of the genomic RNA and the transcription of a so-called nested set of subgenomic mRNAs. Seven subgenomic mRNAs have been identified in MHV-infected cells, and they encode the structural proteins S, M, E, and N (and sometimes HE), two proteins of unknown function (encoded by mRNAs 4 and 5), and a putative cyclic phosphodiesterase (encoded by mRNA2) (31, 32).

An important tool in the analysis of any virus is the ability to alter the viral genome in a prescribed manner. This reverse genetic approach can be used to study the roles of specific gene products in viral replication or pathogenesis and, in the longer term, genetically attenuated viruses that are potential vaccine candidates can be produced. In 1992, Masters and colleagues developed a reverse genetic system for MHV based upon a procedure known as targeted recombination (15, 23). This approach has been very successful but, for technical reasons, has not yet been extended to include mutagenesis of the replicase gene (4). More recently, Yount and colleagues have developed a system based on in vitro-ligated MHV cDNA fragments (6, 39). However, although the systematic assembly of seven cDNAs by in vitro ligation is feasible, the amount of in vitro-transcribed recombinant MHV genome obtained by this method is small. Thus, the system precludes applications where large amounts of in vitro-transcribed coronavirus genome or vector RNAs are required. Moreover, as reported previously, we have observed instability in bacterially cloned coronavirus cDNAs (34).

Here, we report an alternative reverse genetic system for MHV based upon the use of vaccinia virus as a eukaryotic cloning system. This system has proven to be useful for the stable cloning and propagation of full-length cDNAs of group I (human coronavirus [HCoV] 229E) and group III (avian infectious bronchitis coronavirus) coronaviruses (2, 34). Furthermore, this system enables the production of large amounts of in vitro transcripts using recombinant vaccinia virus genomes as a template DNA. Importantly, our reverse genetic system for MHV is based upon a strain of MHV-A59 that grows to high titers in cell culture and produces encephalitis and hepatitis in the natural host. We show here that, using the vaccinia virus-based system, we obtain recombinant viruses that are phenotypically identical to the parental MHV-A59 laboratory strain used to construct the genomic cDNA.

## MATERIALS AND METHODS

**Viruses and cells.** L2 and 17 clone 1 (17Cl-1) mouse fibroblast cells (33) and HeLa-D980R cells (14) were cultured at 37°C in Dulbecco's modified Eagle's medium supplemented with 10% fetal bovine serum (FBS), penicillin (100 U/ml), and streptomycin (100 μg/ml). Monkey kidney (CV-1) cells and baby hamster kidney (BHK-21) cells were obtained from the European Collection of Cell Cultures and cultured in minimal essential medium supplemented with HEPES (25 mM), 5% FBS, and antibiotics. The Albany strain of MHV-A59 (33) was plaque purified and propagated in 17Cl-1 cells with titers of $10^7$ to $10^9$ PFU/ml. Plaque assays were done using 17Cl-1 cells as described previously (29). Vaccinia virus (WR strain), vaccinia virus recombinants, and fowlpox virus were propagated, titrated, and purified as described previously (34).

**Cloning of full-length MHV-A59 cDNA.** A plaque-purified, low-passage stock of MHV-A59 was produced, and the genomic RNA was isolated. This RNA was then used to construct a set of 12 plasmid clones containing MHV-derived cDNAs encompassing nucleotides 1 to 22744. Subsequent ligation of the stable cDNA clones resulted in the generation of two plasmid clones, designated p5′Sac and pSap2ex, that were used for the insertion of the full-length MHV cDNA into the vaccinia virus genome. The plasmid p5′Sac contains an EagI site and a bacteriophage T7 RNA polymerase promoter upstream of the cloned MHV cDNA corresponding to the MHV-A59 nucleotides 1 to 4937. The plasmid pSap2ex contains a cDNA insert corresponding to the MHV-A59 nucleotides 14408 to 22744, including a modification at nucleotides 22738 to 22744 to generate an artificial RsrII restriction site. The plasmid pMH49 (kindly provided by Paul Masters, Wadsworth Center, Albany, N.Y.) (17) was used as a basis to construct a plasmid, designated pMHe-link, that contains a cDNA insert corresponding to the MHV-A59 nucleotides 22744 to 31335 and a synthetic poly(A) sequence. pMHe-link contains two modifications compared to pMH49. First, an EagI recognition sequence corresponding to the MHV-A59 nucleotides 29012-CGGCCG-29017 was changed to 29012-CCGCCG-29017 (the changed nucleotide is underlined), and second, an EagI site was inserted downstream of the synthetic poly(A) sequence. A cDNA fragment corresponding to the MHV-A59 nucleotides 4932 to 14418 was amplified by reverse transcription (RT)-PCR from poly(A)-containing RNA from MHV-A59-infected 17Cl-1 cells using RT-PCR as described previously (36).

To clone a full-length cDNA of MHV-A59 into the vaccinia virus genome, four cDNA fragments were prepared (Fig. 1). Fragment 1 resulted from cleavage of p5′Sac with EagI and XmaI, treatment with alkaline phosphatase, and agarose gel purification of the 5.0-kbp fragment. Fragment 2 was prepared by RT-PCR as described above, cleaved with XmaI and SapI, and purified to remove smaller DNA fragments. Fragment 3 resulted from cleavage of pSap2ex with SapI and RsrII and agarose gel purification of the 8.3-kbp fragment. Fragment 4 resulted from cleavage of pMHe-link with RsrII and EagI, treatment with alkaline phosphatase, and agarose gel purification of the 8.6-kbp fragment. A mixture of 5 μg of DNA containing equimolar amounts of fragments 1 to 4 was ligated in vitro, and the resulting ligation products (containing full-length MHV cDNA fragments) were then ligated to NotI-cleaved vNotI/tk vaccinia virus DNA (24) in the presence of NotI enzyme. The ligation products were transfected without further purification into fowlpox virus-infected CV-1 cells, and recombinant vaccinia viruses were isolated as described previously (34).

**Repair of the MHV-A59 full-length cDNA in the vaccinia virus genome.** To repair RT-PCR-introduced nucleotide changes in the full-length MHV-A59 cDNA contained in vaccinia virus clone vMHV-E6, four rounds of vaccinia virus-mediated homologous recombination were done using the *Escherichia coli* guanine phosphoribosyltransferase (*gpt*) gene as a marker for positive or negative selection (13) (Fig. 2). The plasmid pMHVexI is based on the plasmid pGPT-1 (containing the *gpt* gene) (13) and two cDNA inserts corresponding to the MHV-A59 nucleotides 4779 to 5444 and 14430 to 15035 cloned upstream and downstream of the *gpt* gene, respectively. The plasmid pMHV-G1 is based on the plasmid pMini184-pl (a low-copy-number plasmid, kindly provided by Günther Keil, Federal Research Centre for Virus Diseases of Animals, Insel Riems, Germany) and contains a cDNA insert corresponding to the MHV-A59 nucleotides 4779 to 7614. The plasmid pMHV-G4 is based on the plasmid pMini184-pl and contains a cDNA insert corresponding to the MHV-A59 nucleotides 13055 to 15035. pMHVexII is based on the plasmid pGPT-1 and a cDNA insert corresponding to the MHV-A59 nucleotides 7027 to 10236 cloned upstream of the *gpt* gene. RT-PCR G3 was prepared from poly(A)-containing RNA from MHV-A59-infected 17Cl-1 cells using the oligonucleotide Pr44 (5′-AGAGTTG AACAATCATTGCGGTCA-3′) as a primer for the RT reaction and oligonu-

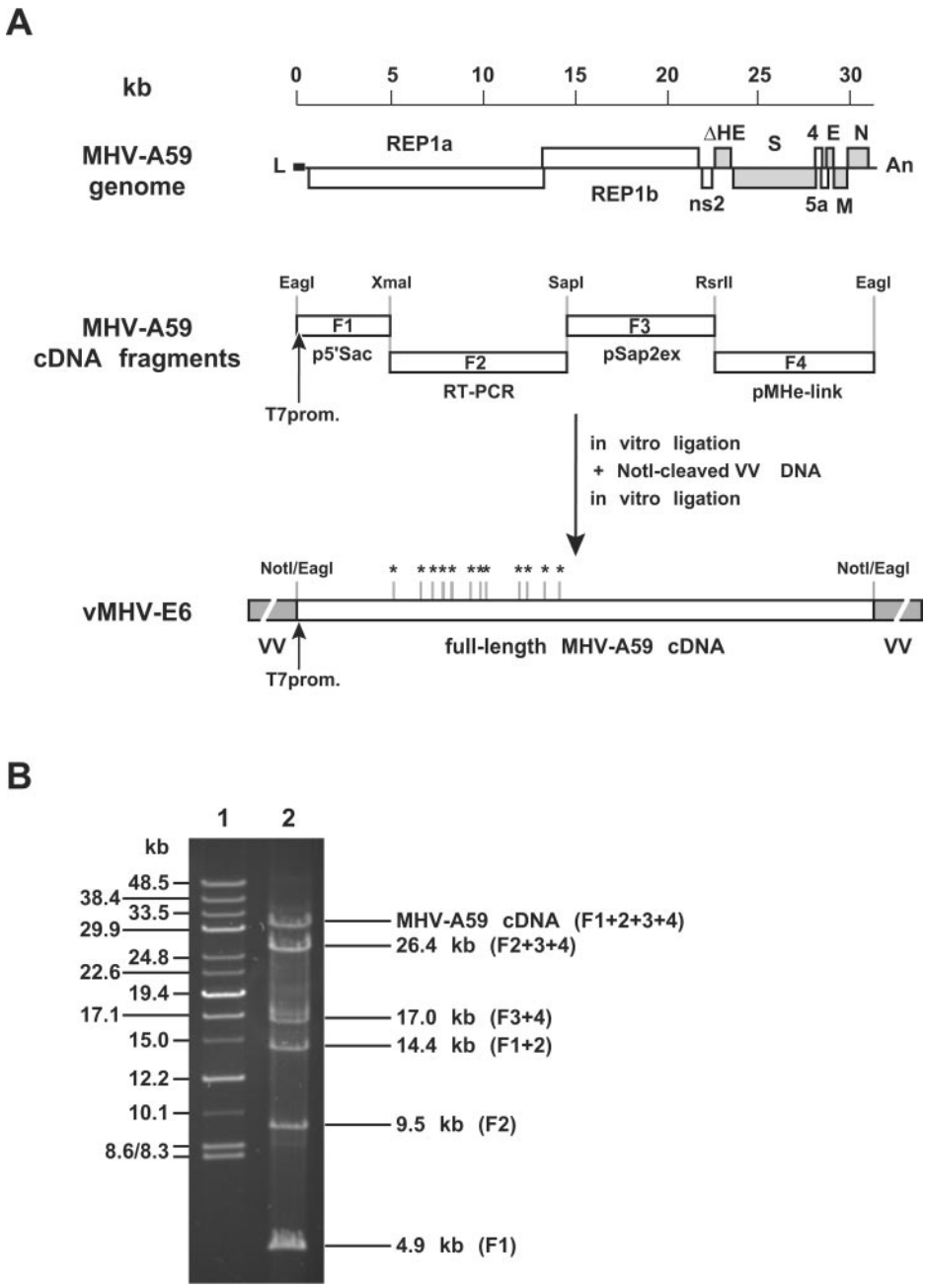


FIG. 1. Assembly of full-length MHV-A59 cDNA by in vitro ligation. (A) The structural relationship of the MHV-A59 genome, MHV-A59-derived cDNA fragments, and full-length cDNA is shown. Four cDNA fragments (F1 to F4), derived from p5′Sac (F1), RT-PCR from MHV-A59 RNA (F2), pSap2ex (F3), and pMHe-link (F4), are assembled by in vitro ligation using appropriate restriction sites as indicated. Also shown is the position of the bacteriophage T7 RNA polymerase promoter (prom.) sequence in fragment F1. The full-length MHV-A59 cDNA is inserted into the vaccinia virus vNotI/tk genome by ligation of full-length MHV-A59 cDNA containing EagI-cleaved DNA ends with NotI-cleaved vNotI/tk genomic DNA (VV). The positions of nucleotide changes introduced by RT-PCR fragment F2 are indicated (*). (B) Pulsed-field gel electrophoresis analysis of the ligation reaction mixture containing fragments F1 to F4. Reaction products corresponding to the full-length MHV-A59 cDNA fragment, intermediate reaction products, and inserted cDNA fragments are indicated.

cleotides MXho12000up (5′-ACGTGCTCGAGTTGTGTTGCTTAATTGCCT CCAGCAC-3′) and Pr43 (5′-CTGGCACAGGGTACAAGACGGGCA-3′) as primers for the PCR. The resulting 1.6-kbp cDNA fragment corresponded to the MHV-A59 nucleotides 12010 to 13648. RT-PCR G2 was prepared from poly(A)-containing RNA from MHV-A59-infected 17Cl-1 cells using the oligonucleotide Pr41 (5′-ATACACAATCTTACCCGTGCCAGT-3′) as a primer for the RT reaction and oligonucleotides Pr91 (5′-TGTGGTTGTTCTCTTACTGCCGCA-3′) and Pr40 (5′-TTGCATTCAAAGGTACACAACCCTT-3′) as primers for the PCR. The resulting 2.7-kbp cDNA fragment corresponded to the MHV-A59 nucleotides 9890 to 12607.

CV-1 cells ($5 \times 10^5$) were infected with recombinant vaccinia viruses at 10 PFU/cell, followed by transfection of 5 μg of DNA 1 h postinfection using Lipofectin transfection reagent (Invitrogen). Two days later, the cells were harvested and recombinant vaccinia viruses were isolated by three rounds of plaque

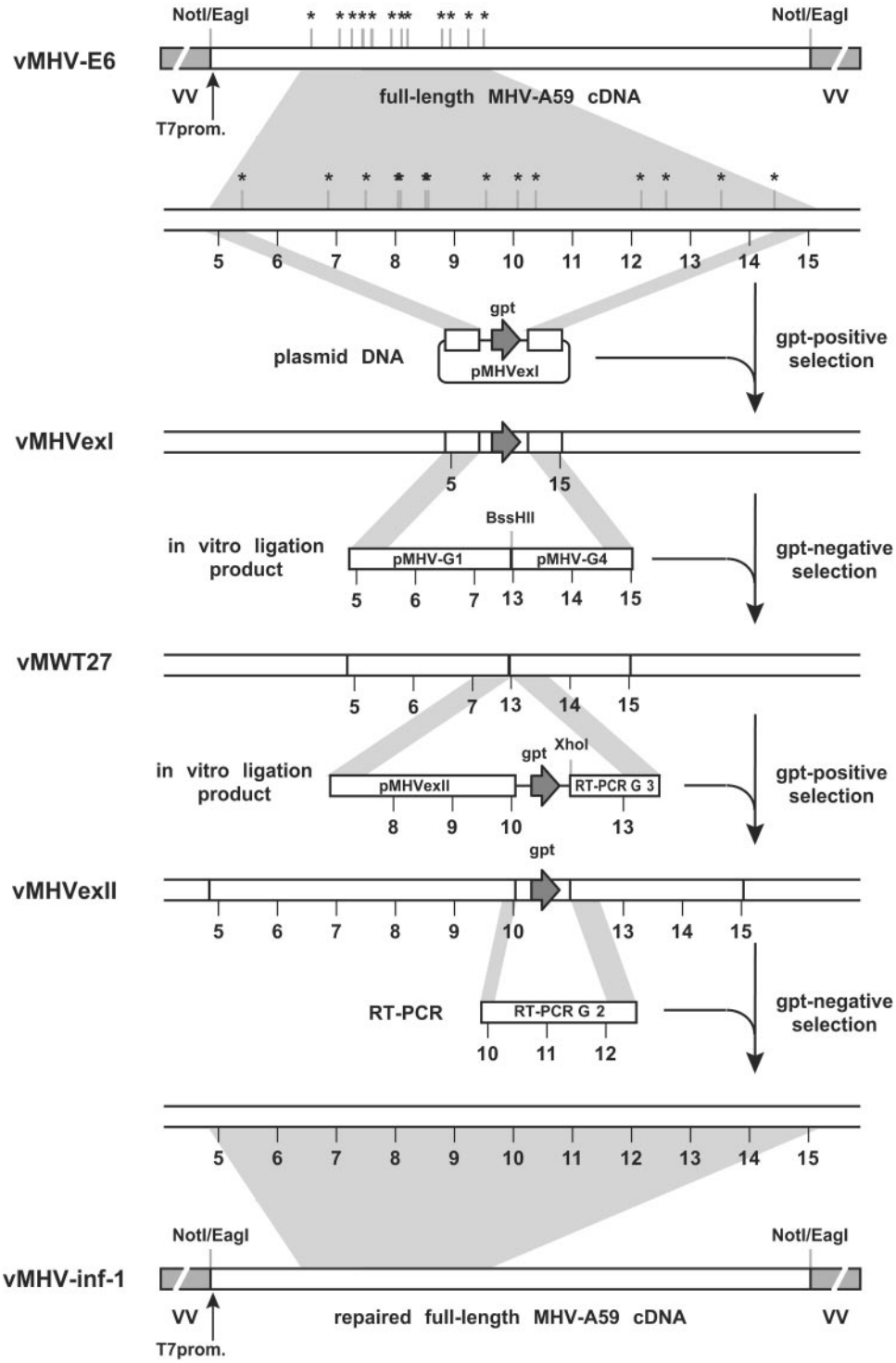


FIG. 2. Repair of cloned full-length MHV-A59 cDNA. The positions of nucleotide changes within the cloned MHV-A59 cDNA of recombinant vaccinia virus (VV) vMHV-E6 are shown (*). The sequence corresponding to MHV-A59 nucleotides 4779 to 15035 containing these changes has been replaced by the MHV-A59 consensus sequence using four rounds of vaccinia virus-mediated homologous recombination with *gpt*-positive or -negative selection conditions as indicated. Also shown are plasmid DNAs, RT-PCR products, and in vitro ligation products that were used for homologous recombination. The numbers depicted on DNA fragments correspond to the positions of the MHV-A59 genome sequence in kilobases.

purification with *gpt*-positive or *gpt*-negative selection using CV-1 and HeLa-D980R cells, respectively. The strategy shown in Fig. 2 demonstrates that recombinant vaccinia virus vMHVexI was isolated after homologous recombination of vMHV-E6 with plasmid pMHVexI using *gpt*-positive selection. Recombinant vaccinia virus vMWT27 was isolated after homologous recombination with a ligation product comprised of BssHII-cleaved plasmid pMHV-G1 and BssHII-cleaved plasmid pMHV-G4 using *gpt*-negative selection. Recombinant vaccinia virus vMHVexII was isolated after recombination of vMWT27 with a ligation product comprised of Xho-cleaved plasmid pMHVexII and Xho-cleaved RT-PCR G3 using gpt-positive selection. Finally, recombinant vaccinia virus vMHV-inf-1 was isolated after recombination of vMWT27 with RT-PCR G2 using *gpt*-negative selection.

**Sequencing and Southern blot analysis.** All plasmid DNAs containing MHV-derived cDNAs were verified by sequence analysis. Recombinant vaccinia clones vMHVexI, vMWT27, and vMHVexII were analyzed by Southern blotting, and the regions involved in vaccinia virus-mediated homologous recombination were verified by sequence analysis. Recombinant vaccinia viruses vMHV-E6 and vMHV-inf-1 were verified by Southern blotting and by sequence analysis of the entire MHV-derived cDNA insert.

**Rescue of recombinant MHV-inf-1.** A regulatable cell line expressing the MHV-A59 nucleocapsid protein was constructed for the rescue of recombinant MHV-inf-1. BHK-21 cells were transfected with 5 μg of plasmid $pcEF_{Tet\text{-}On}$/NEO (28), and a stable cell line, designated BHK-Tet/On, that expresses the Tet-activator protein rtTA was selected using G418 (400 to 800 μg/ml). BHK-Tet/On cells were transfected with 2.5 μg of plasmid pTRE-MN and 2.5 μg of plasmid pTK-Hyg (Clontech), and a stable cell line, BHK-MHV-N, expressing the MHV-A59 nucleocapsid protein in the presence of doxycycline was selected with hygromycin B (300 μg/ml). To construct the plasmid pTRE-MN, the MHV-A59 nucleocapsid gene was amplified from poly(A)-containing RNA from MHV-A59-infected 17Cl-1 cells by PCR using the oligonucleotide primers Sac-MN-ATG (5′-ACGTAGAGCTCACCATGTCTTTTGTTCCTGGGCAAGAA AATGC-3′) and Bam-MN-Stop (5′-ACGTGGATCCTTACACATTAGAGTC ATCTTCTAACC-3′). The PCR product was cleaved with SacII and BamHI and ligated into the SacII- and BamHI-cleaved plasmid pTRE (Clontech).

DNA from purified vaccinia virus vMHV-inf-1, or total DNA from $10^6$ vaccinia virus vMHV-inf-1-infected BHK-21 cells, was used as a template for the bacteriophage T7 RNA polymerase in the presence of m7G(5′)ppp(5′)G cap analog, as described previously (34). MHV-inf-1 in vitro transcripts (10 μg) were electroporated into BHK-MHV-N cells or, together with 5 μg of in vitro-transcribed RNA encoding the MHV N protein, into BHK-21 cells as described previously (35). The cells were then seeded out with a fourfold excess of 17Cl-1 cells. After 16 h, the cell culture supernatant containing recombinant MHV-inf-1 was collected for further analysis.

**Analysis of MHV RNA synthesis in cell culture.** 17Cl-1 cells were infected with MHV at 50 to 100 PFU/cell at 37°C. Following infection, the cells were labeled with [$^3$H]uridine by incubation in Dulbecco's modified Eagle's medium supplemented with 6% FBS and containing 50 μCi of [$^3$H]uridine/ml and 20 μg of dactinomycin/ml. The cells were solubilized with 5% lithium dodecyl sulfate and 200 μg of proteinase K/ml, and a sample of $5 \times 10^4$ cells was analyzed by electrophoresis on a nondenaturing 1% agarose gel (29).

**Mice and virulence assays.** All animal experiments used 4-week-old virus-free C57BL/6 mice (National Cancer Institute, Bethesda, Md.). The mice were anesthetized by inhalation of methoxyflurane. A total volume of 25 μl, containing the virus diluted in phosphate-buffered saline (PBS) with 0.75% bovine serum albumin, was injected intracranially (i.c.) into the left cerebral hemisphere of each mouse. Virulence assays were performed by i.c. inoculation of groups of 10 mice with serial 10-fold dilutions of viruses, as previously described (3). The mice were examined for signs of disease or death on a daily basis for up to 30 days postinfection. All animal experiments adhered to National Institutes of Health guidelines for laboratory animal facilities and care.

**Histological analysis.** Mice were infected i.c. with 1,000 PFU, and two mice per time point were sacrificed at various times (days 1, 3, 5, and 7) postinfection. After intracardiac perfusion with sterile PBS, brains and livers were removed and samples of brain and liver were frozen at −80°C to be analyzed later for viral titers by plaque assays. Half of the brain and a portion of the liver were used for histological analysis (perfused with 10% buffered formalin, paraffin embedded, and stained with hematoxylin and eosin [HE]). For assessment of demyelination, mice were infected with 1,000 PFU of either MHV-A59 or MHV-inf-1/cell. Ten mice infected with MHV-A59 and nine mice infected with MHV-inf-1 were sacrificed 30 days postinfection and underwent intracardiac perfusion with PBS, followed by 10% buffered formalin. The spinal cords were removed, formalin fixed, and paraffin embedded. Four to six transverse sections of cervical, thoracic, and lumbar levels of the cord were stained with Luxol fast blue, and the number of quadrants of cord containing demyelination were counted as a fraction of the total number of cord quadrants evaluated in each individual mouse (21)

**Nucleotide sequence accession number.** The GenBank accession number of the sequence reported in this paper is AY700211.

## RESULTS

**Cloning of full-length MHV-A59 cDNA.** Vaccinia virus has proven to be a suitable vector system for the stable propagation of full-length cDNAs from HCoV-229E and avian infectious bronchitis coronavirus, with genome sizes of 27.3 and 27.6 kb, respectively. Since the genome of MHV-A59 is considerably larger (31.3 kb), we first asked whether cDNA of this size could be stably propagated in vaccinia virus vectors. Thus, we assembled a full-length MHV-A59 cDNA by in vitro ligation of four DNA fragments, one of which was generated by RT-PCR (Fig. 1). The 9.5-kbp RT-PCR-derived fragment corresponds to a region within the MHV-A59 genome that was difficult to maintain as a plasmid in bacterial hosts, and it was expected that the RT-PCR fragment would give rise to multiple PCR-derived nucleotide changes in the cloned cDNA. As illustrated in Fig. 1B, a product comprised of all four DNA fragments and corresponding to the MHV-A59 genome was easily detectable after pulsed-field agarose gel electrophoresis of the ligation reaction mixture. This fragment was then inserted, again by in vitro ligation, into the vaccinia virus genome, and the products of the reaction were transfected into fowlpox virus-infected CV-1 cells. Although fowlpox virus infection of mammalian cells is abortive, it served here as a helper virus to initiate a productive infection of the noninfectious transfected vaccinia virus DNA. We were able to rescue four recombinant vaccinia virus clones, and Southern blot analysis revealed that all of the clones contained a full-length MHV-A59 cDNA insert (data not shown). The rescued vaccinia virus clones grew to the same titer as the parental vaccinia virus, vNotI/tk, indicating that stable propagation of full-length MHV-A59 cDNA in vaccinia virus is possible. The identity of one clone, designated vMHV-E6, was confirmed by sequence analysis of the entire MHV-derived cDNA. As expected, we encountered multiple nucleotide changes within the RT-PCR-derived region of the cloned MHV-A59 cDNA, whereas the sequences of plasmid-derived regions did not contain any changes.

**Repair of cloned full-length MHV-A59 cDNA.** In order to obtain a vaccinia virus clone containing a cDNA insert with the MHV-A59 consensus sequence, we used vaccinia virus-mediated homologous recombination to repair the RT-PCR-derived nucleotide changes. Four rounds of homologous recombination were done using the *E. coli gpt* as a marker for positive or negative selection, as appropriate. As illustrated in Fig. 2, we used plasmid DNA, in vitro ligation products, and short RT-PCR-derived fragments for homologous recombination with vaccinia virus. First, the vaccinia virus clone vMHVexI was generated from vaccinia virus clone vMHV-E6 by replacing the region corresponding to the MHV-A59 nucleotides 5445 to 14429 by the *gpt* gene. This involved the recombination of vMHV-E6 with plasmid pMHVexI and *gpt*-positive selection. Second, the vaccinia virus clone vMWT-27 was generated when the *gpt* gene was replaced by the MHV-A59-derived sequences 5445 to 7614 and 13055 to 14429. This involved the recombination of vMHVexI with an in vitro ligation product

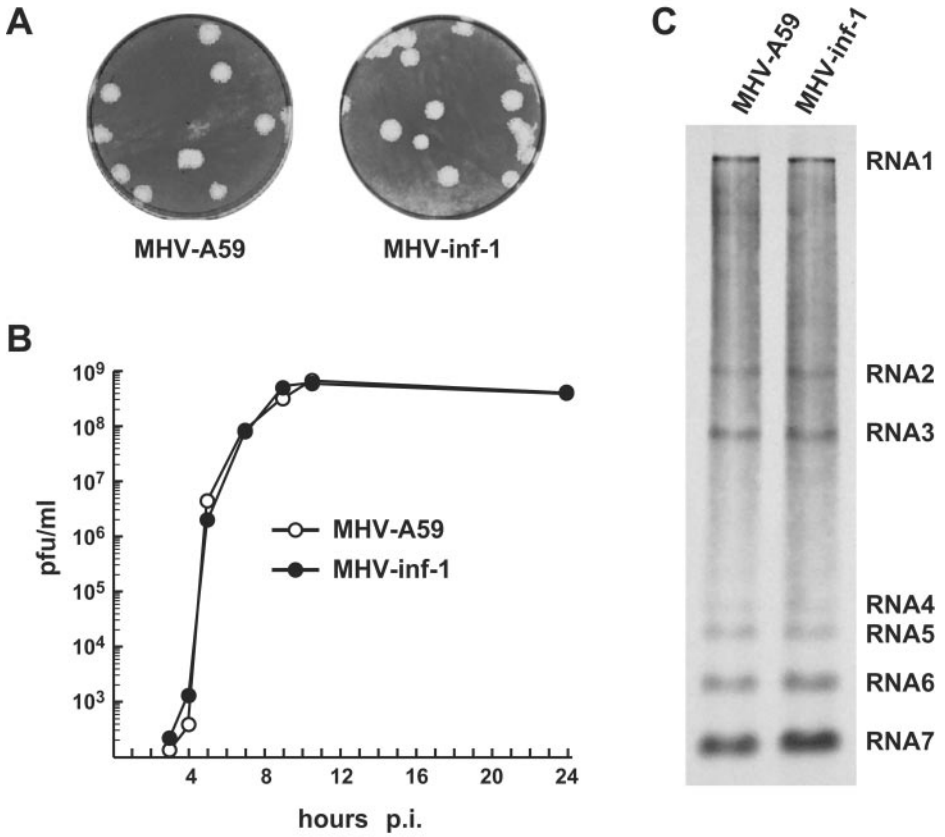


FIG. 3. Analysis of MHV replication in tissue culture. Plaque morphology (A), growth curves (B), and analysis of intracellular [$^3$H]uridine-labeled RNA of parental MHV-A59 and recombinant MHV-inf-1 (C) are shown. p.i., postinfection.

derived from plasmids pMHV-G1 and pMHV-G4 and *gpt*-negative selection. Third, the vaccinia virus clone vMHVexII was generated after recombination of vMWT-27 with a ligation product derived from plasmid pMHVexII (containing the MHV-A59-derived nucleotides 7027 to 10236 and the *gpt* gene) and RT-PCR G3 (containing the MHV-A59-derived nucleotides 12010 to 13648) using *gpt*-positive selection. Finally, using *gpt*-negative selection, the RT-PCR product G2 (containing MHV-A59 nucleotides 9890 to 12607) was used for recombination with vaccinia virus vMHVexII to complete the full-length MHV-A59 cDNA. The identity of the resulting vaccinia virus clone, vMHV-inf-1, was confirmed by Southern blotting and sequence analysis of the entire MHV-A59-derived cDNA insert. The nucleotide sequence of the cloned full-length MHV-A59 cDNA was found to correspond to the authentic MHV-A59 consensus sequence, with the exception of one change that had been specifically introduced by site-directed mutagenesis for cloning purposes (modification of the EagI site in plasmid pMHe-link) and three silent nucleotide changes (MHV-A59 nucleotide 7476, G to A; nucleotide 9246, C to U; nucleotide 12140, G to A) that had been detected in the cloned cDNAs of the plasmids pMHV-G1 (nucleotide 7476) and pMHVexII (nucleotide 9246) and the recombinant vaccinia virus vMHVexII (nucleotide 12140). This result confirms that vaccinia virus genomes can be used to stably maintain and propagate full-length MHV cDNA and, furthermore, that vaccinia virus-mediated recombination represents a powerful method to modify full-length coronavirus cDNAs. We observed in each recombination step that >90% of recombinant clones contained the expected cDNA, and sequencing analysis revealed that vaccinia virus-mediated recombination was also precise at the nucleotide level.

**Rescue of recombinant MHV-inf-1.** After reverse genetic systems for coronaviruses became available, it was shown that the rescue of recombinant coronaviruses is greatly facilitated under conditions that allow N protein expression (2, 39). Accordingly, we found that it was possible to rescue recombinant MHV from cloned cDNA by a number of different methods involving N protein expression. First, full-length MHV-inf-1 RNA was produced by the in vitro transcription of EagI-cleaved vMHV-inf-1 DNA from purified virions. In addition, a synthetic mRNA encoding the MHV nucleocapsid protein was generated by in vitro transcription of MHV-A59 N protein cDNA (V. Thiel, unpublished data). Then, both RNAs were electroporated into BHK-21 cells and the transfected cells were cocultivated with murine 17Cl-1 cells. After 16 h, virus-induced syncytia were detectable in areas predominantly occupied by 17Cl-1 cells. The supernatant was transferred to fresh 17Cl-1 cells, and extensive cytopathic effect became apparent after 10 to 16 h. Recombinant MHV-A59 was readily isolated from the culture supernatant. Second, we produced in vitro transcripts of MHV-inf-1 RNA using a template derived from total DNA isolated from vMHV-inf-1-infected BHK-21 cells. Electroporation of this RNA into BHK-21 cells, together with

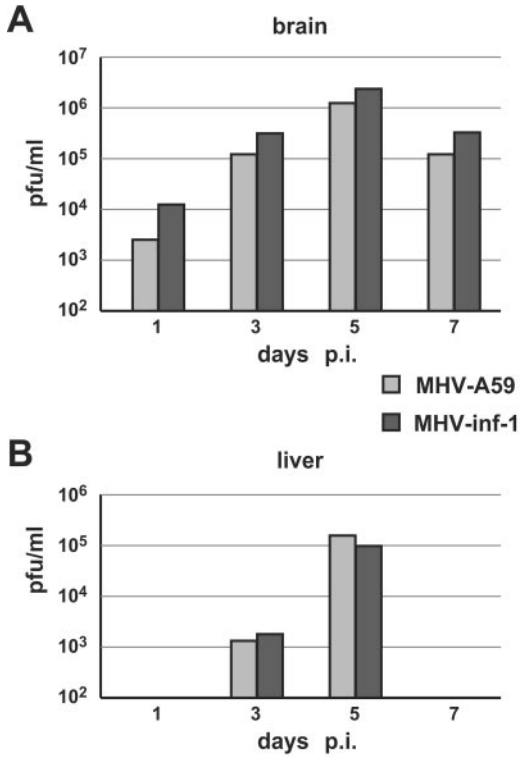


FIG. 4. Virus replication in mice. Shown are viral titers in the brains and livers of 4-week-old C57BL/6 mice infected with either parental MHV-A59 or recombinant MHV-inf-1. Viral titers were examined by plaque assays on L2 cells. Each time point represents the average titer of the organs of two mice. p.i., postinfection.

nucleocapsid protein-encoding RNA, and subsequent cocultivation with 17Cl-1 cells also gave rise to recombinant MHV. Finally, we found that recombinant MHV could be rescued by electroporation of full-length MHV-inf-1 RNA into a stable BHK-21-derived cell line expressing the MHV-A59 nucleocapsid protein (BHK-MHV-N) cocultivated with 17Cl-1 cells. We think it is important to note that the use of a stable cell line expressing the MHV nucleocapsid protein not only facilitates the rescue procedure but also allows the phenotypic analysis of recombinant MHV in transfected cells (Thiel, unpublished).

**Replication of recombinant MHV-inf-1 in cell culture.** In order to confirm that the rescued recombinant MHV, MHV-inf-1, has the same in vitro replication phenotype as the parental virus, we compared the plaque morphology, single-cycle replication kinetics, and patterns of intracellular viral RNA synthesis. As shown in Fig. 3, the recombinant virus is indistinguishable from the parental virus. It replicates to the same titers in cell culture and has the same plaque morphology. In cells infected with either virus, the same amounts and proportions of genomic and subgenomic mRNAs are synthesized with the same kinetics.

**Virulence of recombinant MHV-inf-1 in mice.** The virulence of MHV-inf-1 was compared to that of MHV-A59. Groups of 10 4-week-old C57BL/6 mice were infected i.c. with serial 10-fold dilutions of the viruses. The experiments with the critical doses of 500 and 5,000 PFU were performed twice with two separate groups of mice. In the MHV-inf-1-infected mice, the mortality rate of mice infected with 500 PFU was 0 in 10 mice in each experiment, whereas 5,000 PFU produced mortality rates of 6 in 10 and 7 in 10, respectively, and the dose of 50,000 PFU produced mortality of 10 in 10. In mice infected with MHV-A59, the dose of 500 PFU produced 0 in 10 mortality in each experiment, while 5,000 PFU produced mortality of 4 in 10 and 5 in 10, respectively, and 50,000 PFU killed 5 of 5 mice. Thus, the lethal dose that killed 50% of the mice ($LD_{50}$) with MHV-A59 was 5,000 PFU per mouse. In comparison, MHV-inf-1 was slightly more virulent, and the $LD_{50}$ of MHV-inf-1 was ~2,000 PFU per mouse. The differences between the mortality rates of the two viruses are not statistically significant.

**Replication of MHV-inf-1 in mouse tissues.** Following i.c. infection of 4-week-old C57BL/6 mice with 1,000 PFU of either MHV-inf-1 or MHV-A59, the replication of the virus in brains and livers was assessed by plaque assays (Fig. 4). Viral titers of both MHV-inf-1 and MHV-A59 peaked at day 5 and declined thereafter. The viral titers of both infections were similar, with slightly higher titers evident in MHV-inf-1-infected mouse brains.

**Histopathology of mouse brain and liver.** Light microscopy of HE-stained sections of liver during acute infection showed foci of necrosis and inflammatory cells representing acute hepatitis (Fig. 5D). MHV-A59-infected mice and MHV-inf-1-infected mice showed similar pathologies. Both groups of mice were infected with a dose of 1,000 PFU per animal. During acute infection with MHV-A59, brain tissues showed acute meningoencephalitis, including mononuclear inflammatory cellular infiltration in perivascular spaces and slight parenchymal infiltration. In addition, there was microglial and glial proliferation and neuronophagia (Fig. 5A to C). The affected regions of the brain were as previously described (20, 21). Sections of the brains of mice infected with MHV-inf-1 exhibited the same pathology at the same distribution and intensity. The combined pathological score (on the basis of mild, moderate, and severe disease [9]) of all animals infected with MHV-A59 was not statistically different from that of animals infected with MHV-inf-1 in both liver and brain histology.

**Chronic demyelination.** The hallmark of MHV-A59 infection is the ability to produce chronic demyelination similar to the human disease multiple sclerosis. Infection of 4-week-old C57BL/6 mice with MHV-inf-1 caused an amount of demyelination at 30 days postinfection (Fig. 5E) similar to that in mice infected with the same dose (1,000 PFU) of MHV-A59. Demyelination was found in all mice ($n = 9$) in 65 out of 180 quadrants of spinal cord sections (36%). MHV-A59 infection with 1,000 PFU of virus produced demyelination in 100% of the mice (10 of 10) in 77 of 196 quadrants of spinal cord sections examined (39%). The differences between the rates of demyelination in the two viruses are not statistically significant.

## DISCUSSION

In this study, we describe a genetic system based on a cloned full-length DNA copy of the MHV-A59 genome. We show that this cDNA can be stably propagated using a vaccinia virus vector and that it is amenable to mutagenesis via vaccinia virus-mediated homologous recombination. The parental MHV-A59 strain that we chose for the construction of the

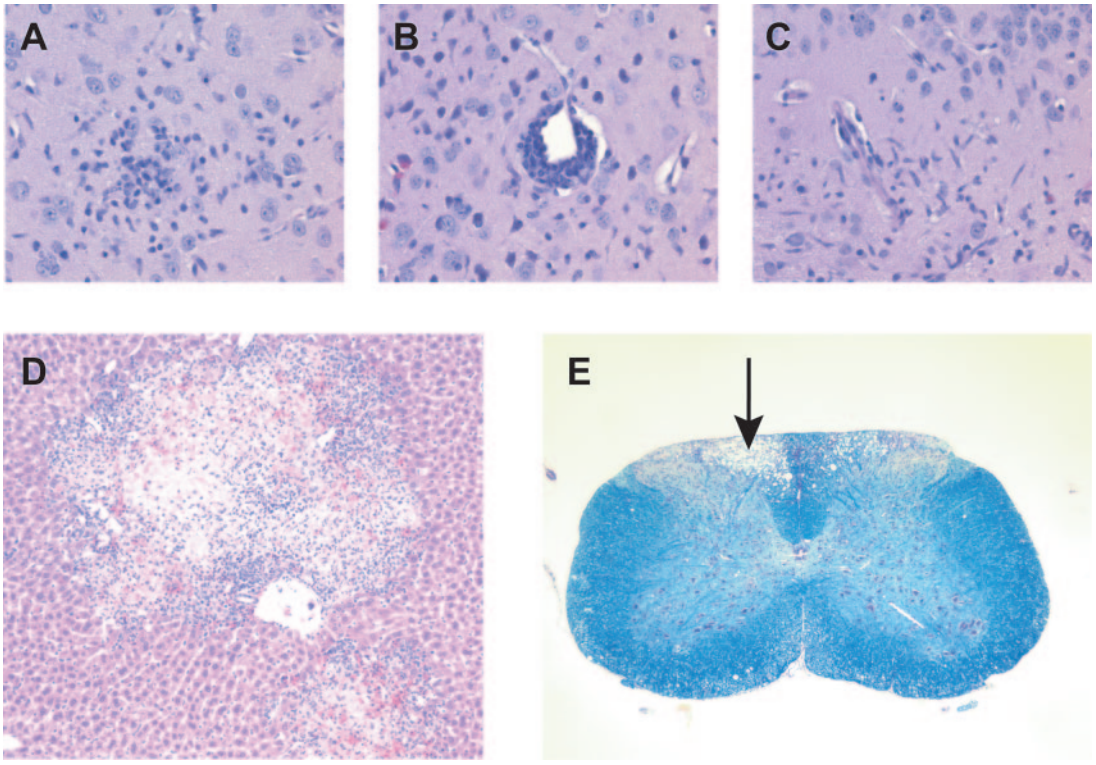


FIG. 5. Histopathology of mouse brain, spinal cord, and liver following infection with recombinant MHV-inf-1. Brain sections (A to C) at 7 days postinfection show acute encephalitis with microglial nodules (A), perivascular mononuclear cellular infiltration in brain parenchyma (B) and meninges, and microglial proliferation (C). (D) Liver sections at 5 days postinfection show numerous foci of necrosis and inflammation throughout the liver parenchyma. (E) Sections of spinal cord at 30 days postinfection show multiple demyelinating lesions (arrow) in the white matter. Panels A to C are HE stained at ×400 magnification; plate D is an HE stain at ×200 magnification; panel E is a Luxol fast blue stain for myelin at ×50 magnification.

full-length cDNA produces high titers of virus in tissue culture and is fully pathogenic in mice. The recombinant MHV derived from the cDNA copy of this virus has the same phenotype as the parental virus in vitro and in vivo. Therefore, the reverse genetic system we describe here represents a versatile and universal tool to study all aspects of MHV molecular biology and pathogenesis. Also, the system we describe will provide a starting point for the generation of multigene RNA vectors based on MHV. The concept of coronavirus multigene vectors has been developed for HCoV-229E with the specific goal of transducing human antigen-presenting cells in order to mediate heterologous gene expression and induce both T-cell and antibody responses to multiple antigens (35). Recently, it has been shown that MHV-A59 can infect murine dendritic cells (38), indicating that MHV-based vectors with characteristics similar to their HCoV-229E counterparts can be produced. This finding should encourage the establishment of a murine model for the evaluation of coronavirus multigene vaccines in preclinical trials.

In addition, we describe in this paper some technical improvements that will facilitate the mutagenesis and rescue of recombinant coronaviruses in the vaccinia virus vector system. For example, we show that the use of vaccinia virus-mediated homologous recombination is not dependent on cloned plasmids as donor DNA. We demonstrate that fragments derived from RT-PCR products, or even in vitro-ligated DNA fragments, can be used for homologous recombination. This is of particular interest in relation to the mutagenesis of regions within the coronavirus genome that are difficult to clone and maintain in plasmid DNAs. Second, we describe alternative procedures for the rescue of recombinant coronaviruses from cDNAs cloned in vaccinia virus vectors. For example, we have shown that it is no longer required to grow large stocks of purified vaccinia viruses in order to prepare DNA templates for the in vitro transcription of a full-length MHV genome. Our results show that as few as $10^6$ vaccinia virus-infected cells grown in a six-well dish suffice for the preparation of total DNA suitable for the generation of infectious full-length MHV RNA. Finally, we have shown that a BHK-21-derived cell line expressing the MHV nucleocapsid protein (BHK-MHV-N) facilitates the efficient rescue of recombinant MHV. This obviates the need to coelectroporate genomic RNA and synthetic mRNA encoding the nucleocapsid protein in order to rescue recombinant virus and, more importantly, allows the analysis of coronavirus MHV RNA synthesis in transfected cells.

MHV represents by far the best-studied coronavirus. Much of our knowledge of the molecular biology and pathogenesis of coronavirus infections has been elucidated using MHV, and in particular, reverse genetic approaches based on targeted recombination have contributed greatly to our present understanding of coronavirus biology (4, 5, 10, 26). The development of a vaccinia virus vector-based reverse genetic system for

MHV will add further impetus to this research. However, the relevance of MHV as a model of coronavirus infection has also been significantly enhanced as a result of the identification of SARS CoV as the causative agent of SARS (27). Specifically, phylogenetic analysis has revealed a relationship of SARS CoV to group II coronaviruses (which includes MHV) (32), and given the striking homology of many coronavirus genes, particularly within the same phylogenetic group, the MHV system should provide the opportunity to study many aspects of SARS CoV replication without the need to work under the most stringent containment conditions. For example, it has been shown already that the SARS CoV 3′ nontranslated region, which includes predicted *cis*-acting RNA elements required for genome replication, can function in chimeric MHV-SARS CoV genomes (11). This result supports a functional relationship of SARS CoV to other group II coronaviruses and indicates that SARS CoV *cis*-acting RNA elements can interact with MHV replicative enzymes. Consequently, the analysis of MHV replication will ultimately lead to new insights into the replication of SARS CoV, and this will include the analysis of candidate inhibitors that target replicative functions. Thus, the efficacy of putative SARS CoV replicase inhibitors can be assessed in well-established MHV animal models, and the evolution of resistance to such inhibitors can be studied in MHV models of infection. In this context, reverse genetic systems for MHV can play an essential role in the development of strategies to prevent and control coronavirus infections, including SARS.

## ACKNOWLEDGMENTS

We are grateful to Paul Masters (Wadsworth Center, Albany, N.Y.), Geoffrey L. Smith (Imperial College, London, United Kingdom), Norbert Tautz (Justus Liebig University, Giessen, Germany), and Günther Keil (Federal Research Institute for Animal Health, Insel Riems, Germany) for valuable plasmid constructs and cells.

This study was supported by the German Research Council (DFG), the Gebert-Rüf Foundation, and the Swiss Cancer League.

## REFERENCES

1. **Barthold, S. W., D. S. Beck, and A. L. Smith.** 1993. Enterotropic coronavirus (mouse hepatitis virus) in mice: influence of host age and strain on infection and disease. Lab. Anim. Sci. **43:**276–284.
2. **Casais, R., V. Thiel, S. G. Siddell, D. Cavanagh, and P. Britton.** 2001. Reverse genetics system for the avian coronavirus infectious bronchitis virus. J. Virol. **75:**12359–12369.
3. **Das Sarma, J., L. Fu, J. C. Tsai, S. R. Weiss, and E. Lavi.** 2000. Demyelination determinants map to the spike glycoprotein gene of coronavirus mouse hepatitis virus. J. Virol. **74:**9206–9213.
4. **de Haan, C. A., P. S. Masters, X. Shen, S. Weiss, and P. J. Rottier.** 2002. The group-specific murine coronavirus genes are not essential, but their deletion, by reverse genetics, is attenuating in the natural host. Virology **296:**177–189.
5. **de Haan, C. A., L. van Genne, J. N. Stoop, H. Volders, and P. J. Rottier.** 2003. Coronaviruses as vectors: position dependence of foreign gene expression. J. Virol. **77:**11312–11323.
6. **Denison, M. R., B. Yount, S. M. Brockway, R. L. Graham, A. C. Sims, X. Lu, and R. S. Baric.** 2004. Cleavage between replicase proteins p28 and p65 of mouse hepatitis virus is not required for virus replication. J. Virol. **78:**5957–5965.
7. **Donnelly, C. A., A. C. Ghani, G. M. Leung, A. J. Hedley, C. Fraser, S. Riley, L. J. Abu-Raddad, L. M. Ho, T. Q. Thach, P. Chau, K. P. Chan, T. H. Lam, L. Y. Tse, T. Tsang, S. H. Liu, J. H. Kong, E. M. Lau, N. M. Ferguson, and R. M. Anderson.** 2003. Epidemiological determinants of spread of causal agent of severe acute respiratory syndrome in Hong Kong. Lancet **361:**1761–1766.
8. **Drosten, C., S. Gunther, W. Preiser, S. van der Werf, H. R. Brodt, S. Becker, H. Rabenau, M. Panning, L. Kolesnikova, R. A. Fouchier, A. Berger, A. M. Burguiere, J. Cinatl, M. Eickmann, N. Escriou, K. Grywna, S. Kramme, J. C. Manuguerra, S. Muller, V. Rickerts, M. Sturmer, S. Vieth, H. D. Klenk, A. D. Osterhaus, H. Schmitz, and H. W. Doerr.** 2003. Identification of a novel coronavirus in patients with severe acute respiratory syndrome. N. Engl. J. Med. **348:**1967–1976.
9. **Fu, L., D. M. Gonzales, J. D. Sarma, and E. Lavi.** 2004. A combination of mutations in the S1 part of the spike glycoprotein gene of coronavirus MHV-A59 abolishes demyelination. J. Neurovirol. **10:**41–51.
10. **Goebel, S. J., B. Hsue, T. F. Dombrowski, and P. S. Masters.** 2004. Characterization of the RNA components of a putative molecular switch in the 3′ untranslated region of the murine coronavirus genome. J. Virol. **78:**669–682.
11. **Goebel, S. J., J. Taylor, and P. S. Masters.** 2004. The 3′ *cis*-acting genomic replication element of the severe acute respiratory syndrome coronavirus can function in the murine coronavirus genome. J. Virol. **78:**7846–7851.
12. **Haring, J., and S. Perlman.** 2001. Mouse hepatitis virus. Curr. Opin. Microbiol. **4:**462–466.
13. **Hertzig, T., E. Scandella, B. Schelle, J. Ziebuhr, S. G. Siddell, B. Ludewig, and V. Thiel.** 2004. Rapid identification of coronavirus replicase inhibitors using a selectable replicon RNA. J. Gen. Virol. **85:**1717–1725.
14. **Kerr, S. M., and G. L. Smith.** 1991. Vaccinia virus DNA ligase is nonessential for virus replication: recovery of plasmids from virus-infected cells. Virology **180:**625–632.
15. **Koetzner, C. A., M. M. Parker, C. S. Ricard, L. S. Sturman, and P. S. Masters.** 1992. Repair and mutagenesis of the genome of a deletion mutant of the coronavirus mouse hepatitis virus by targeted RNA recombination. J. Virol. **66:**1841–1848.
16. **Ksiazek, T. G., D. Erdman, C. S. Goldsmith, S. R. Zaki, T. Peret, S. Emery, S. Tong, C. Urbani, J. A. Comer, W. Lim, P. E. Rollin, S. F. Dowell, A. E. Ling, C. D. Humphrey, W. J. Shieh, J. Guarner, C. D. Paddock, P. Rota, B. Fields, J. DeRisi, J. Y. Yang, N. Cox, J. M. Hughes, J. W. LeDuc, W. J. Bellini, and L. J. Anderson.** 2003. A novel coronavirus associated with severe acute respiratory syndrome. N. Engl. J. Med. **348:**1953–1966.
17. **Kuo, L., G. J. Godeke, M. J. Raamsman, P. S. Masters, and P. J. Rottier.** 2000. Retargeting of coronavirus by substitution of the spike glycoprotein ectodomain: crossing the host cell species barrier. J. Virol. **74:**1393–1406.
18. **Kyuwa, S., S. Shibata, Y. Tagawa, Y. Iwakura, K. Machii, and T. Urano.** 2002. Acute hepatic failure in IFN-gamma-deficient BALB/c mice after murine coronavirus infection. Virus Res. **83:**169–177.
19. **Lai, M. M. C., and K. V. Holmes.** 2001. Coronaviruses, p. 1163–1185. *In* D. M. Knipe, P. M. Howley, D. E. Griffin, R. A. Lamb, M. A. Martin, B. Roizman, and S. E. Straus (ed.), Fields virology. Lippincott, Williams & Wilkins, Philadelphia, Pa.
20. **Lavi, E., P. S. Fishman, M. K. Highkin, and S. R. Weiss.** 1988. Limbic encephalitis after inhalation of a murine coronavirus. Lab. Investig. **58:**31–36.
21. **Lavi, E., D. H. Gilden, Z. Wroblewska, L. B. Rorke, and S. R. Weiss.** 1984. Experimental demyelination produced by the A59 strain of mouse hepatitis virus. Neurology **34:**597–603.
22. **Manaker, R. A., C. V. Piczak, A. A. Miller, and M. F. Stanton.** 1961. A hepatitis virus complicating studies with mouse leukemia. J. Natl. Cancer Inst. **27:**29–51.
23. **Masters, P. S., C. A. Koetzner, C. A. Kerr, and Y. Heo.** 1994. Optimization of targeted RNA recombination and mapping of a novel nucleocapsid gene mutation in the coronavirus mouse hepatitis virus. J. Virol. **68:**328–337.
24. **Merchlinsky, M., and B. Moss.** 1992. Introduction of foreign DNA into the vaccinia virus genome by in vitro ligation: recombination-independent selectable cloning vectors. Virology **190:**522–526.
25. **Narayanan, K., and S. Makino.** 2001. Cooperation of an RNA packaging signal and a viral envelope protein in coronavirus RNA packaging. J. Virol. **75:**9059–9067.
26. **Navas, S., and S. R. Weiss.** 2003. Murine coronavirus-induced hepatitis: JHM genetic background eliminates A59 spike-determined hepatotropism. J. Virol. **77:**4972–4978.
27. **Peiris, J. S., S. T. Lai, L. L. Poon, Y. Guan, L. Y. Yam, W. Lim, J. Nicholls, W. K. Yee, W. W. Yan, M. T. Cheung, V. C. Cheng, K. H. Chan, D. N. Tsang, R. W. Yung, T. K. Ng, and K. Y. Yuen.** 2003. Coronavirus as a possible cause of severe acute respiratory syndrome. Lancet **361:**1319–1325.
28. **Rinck, G., C. Birghan, T. Harada, G. Meyers, H. J. Thiel, and N. Tautz.** 2001. A cellular J-domain protein modulates polyprotein processing and cytopathogenicity of a pestivirus. J. Virol. **75:**9470–9482.
29. **Sawicki, D., T. Wang, and S. Sawicki.** 2001. The RNA structures engaged in replication and transcription of the A59 strain of mouse hepatitis virus. J. Gen. Virol. **82:**385–396.
30. **Siddell, S., D. Sawicki, Y. Meyer, V. Thiel, and S. Sawicki.** 2001. Identification of the mutations responsible for the phenotype of three MHV RNA-negative ts mutants. Adv. Exp. Med. Biol. **494:**453–458.
31. **Siddell, S. G.** 1995. The Coronaviridae. Plenum Press, New York, N.Y.
32. **Snijder, E. J., P. J. Bredenbeek, J. C. Dobbe, V. Thiel, J. Ziebuhr, L. L. Poon, Y. Guan, M. Rozanov, W. J. Spaan, and A. E. Gorbalenya.** 2003. Unique and conserved features of genome and proteome of SARS-coronavirus, an early split-off from the coronavirus group 2 lineage. J. Mol. Biol. **331:**991–1004.
33. **Sturman, L. S., and K. K. Takemoto.** 1972. Enhanced growth of a murine coronavirus in transformed mouse cells. Infect. Immun. **6:**501–507.
34. **Thiel, V., J. Herold, B. Schelle, and S. G. Siddell.** 2001. Infectious RNA transcribed in vitro from a cDNA copy of the human coronavirus genome cloned in vaccinia virus. J. Gen. Virol. **82:**1273–1281.

35. **Thiel, V., N. Karl, B. Schelle, P. Disterer, I. Klagge, and S. G. Siddell.** 2003. Multigene RNA vector based on coronavirus transcription. J. Virol. **77:**9790–9798.
36. **Thiel, V., A. Rashtchian, J. Herold, D. M. Schuster, N. Guan, and S. G. Siddell.** 1997. Effective amplification of 20-kb DNA by reverse transcription PCR. Anal. Biochem. **252:**62–70.
37. **Tsai, J. C., B. D. Zelus, K. V. Holmes, and S. R. Weiss.** 2003. The N-terminal domain of the murine coronavirus spike glycoprotein determines the CEACAM1 receptor specificity of the virus strain. J. Virol. **77:**841–850.
38. **Turner, B. C., E. M. Hemmila, N. Beauchemin, and K. V. Holmes.** 2004. Receptor-dependent coronavirus infection of dendritic cells. J. Virol. **78:**5486–5490.
39. **Yount, B., M. R. Denison, S. R. Weiss, and R. S. Baric.** 2002. Systematic assembly of a full-length infectious cDNA of mouse hepatitis virus strain A59. J. Virol. **76:**11065–11078.
40. **Ziebuhr, J., E. J. Snijder, and A. E. Gorbalenya.** 2000. Virus-encoded proteinases and proteolytic processing in the Nidovirales. J. Gen. Virol. **81:**853–879.